

X-linked H3K27me3 demethylase *Utx* is required for embryonic development in a sex-specific manner

G. Grant Welstead^a, Menno P. Creyghton^{a,1}, Steve Bilodeau^a, Albert W. Cheng^{a,b,c}, Styliani Markoulaki^a, Richard A. Young^{a,b}, and Rudolf Jaenisch^{a,b,2}

^aWhitehead Institute for Biomedical Research, Cambridge, MA 02142; ^bDepartment of Biology, Massachusetts Institute of Technology, Cambridge, MA 02142; and ^cComputational and Systems Biology Program, Massachusetts Institute of Technology, Cambridge, MA 02142

Contributed by Rudolf Jaenisch, June 27, 2012 (sent for review June 8, 2012)

Embryogenesis requires the timely and coordinated activation of developmental regulators. It has been suggested that the recently discovered class of histone demethylases (UTX and JMJD3) that specifically target the repressive H3K27me3 modification play an important role in the activation of “bivalent” genes in response to specific developmental cues. To determine the requirements for UTX in pluripotency and development, we have generated *Utx*-null ES cells and mutant mice. The loss of UTX had a profound effect during embryogenesis. *Utx*-null embryos had reduced somite counts, neural tube closure defects and heart malformation that presented between E9.5 and E13.5. Unexpectedly, homozygous mutant female embryos were more severely affected than hemizygous mutant male embryos. In fact, we observed the survival of a subset of UTX-deficient males that were smaller in size and had reduced lifespan. Interestingly, these animals were fertile with normal spermatogenesis. Consistent with a midgestation lethality, UTX-null male and female ES cells gave rise to all three germ layers in teratoma assays, though sex-specific differences could be observed in the activation of developmental regulators in embryoid body assays. Lastly, ChIP-seq analysis revealed an increase in H3K27me3 in *Utx*-null male ES cells. In summary, our data demonstrate sex-specific requirements for this X-linked gene while suggesting a role for UTY during development.

KDM6A | polycomb

During differentiation and embryogenesis, developmental genes are temporally and spatially regulated by multiple cellular mechanisms. Specific histone modifications such as methylation of lysine residues are associated with either the active or silent state of gene transcription. For example, histone 3 lysine 4 trimethylation (H3K4me3) is commonly found at transcriptional start sites and is generally a mark for transcriptional initiation, whereas histone 3 lysine trimethylation (H3K27me3) is associated with repressed gene expression (1–3). The presence of both H3K4me3 and H3K27me3 at the same gene is termed the “bivalent state” (4). In ES cells, developmental regulators are in a “bivalent state” that creates a poised condition for activation during differentiation (5). To understand the functional role of histone modifications, it is important to understand how bivalent domains are maintained in ES cells and resolved during differentiation.

Although the machinery that deposits the trimethyl modification on histone H3K27, polycomb repressive complex 2 (PRC2), has been studied extensively, the class of enzymes that remove methyl marks from this lysine was only recently identified (6–9). UTX, UTY, and JMJD3 form a family of JmjC-domain containing proteins that specifically demethylate H3K27me3/me2. UTX is encoded on the X chromosome but escapes X inactivation in females and is ubiquitously expressed (10). In males, its homolog on the Y chromosome, UTY, shares similar patterns of expression with some sex-specific differences (11). Both proteins contain tetratricopeptide repeats in their amino terminus that mediate protein–protein interactions, whereas the JmjC domain is located in the C terminus. However, UTY is not active when tested in vitro, although the amino acids critical for demethylase function are conserved (6, 7, 12).

To further understand the events regulating H3K27me3 in ES cells and during development, we generated *Utx*-null ESCs and mutant mice. We demonstrate a significant difference in the phenotype of male and female UTX-deficient embryos. Although a small number of *Utx*-null males survived postnatally, female mutant embryos died at midgestation. The surviving mutant males were smaller than control mice but were fertile with normal spermatogenesis. We derived both male and female UTX-null ES cells from the inner cell mass of blastocysts and show that UTX is dispensable for ES cell self-renewal and germ layer specification consistent with the in vivo phenotype. However, when mutant ES cells were differentiated, differences in gene activation were detected. Furthermore, in the absence of UTX, H3K27me3 levels were increased and H3K4me3 levels were decreased at developmental regulators. Our results demonstrate a requirement for UTX and suggest an important role for its Y-homolog, UTY, in male embryogenesis.

Results

Utx Is Critical for Embryonic Development. To study the function of UTX in ES cells and embryogenesis, male *Utx*^{KO} ES cells were generated by gene targeting of V6.5 ES cells using a “knockout first” construct designed by EUCOMM (Fig. S1A). Correctly targeted cells (*Utx*^{hypp}) displayed hypomorphic expression of UTX, which was completely ablated after Cre addition (*Utx*^{KO}). Conversely, when the cells were treated with Flipase, UTX expression was restored to wild-type levels (*Utx*^{Flix}) (Fig. S1B). All three ES cell lines were injected into blastocysts to generate chimeras. Both the *Utx*^{hypp} and *Utx*^{Flix} ES-cell-injected blastocysts gave rise to chimeras that transmitted the mutant allele.

To generate UTX-null animals, conditional mutant males with the germ-line active Nestin-cre allele (see experimental procedures) were crossed with *Utx*^{KO/wt} females to generate a 1:1:1:1 expected ratio of *Utx*^{wt} and *Utx*^{KO} males and *Utx*^{KO/wt} and *Utx*^{KO/KO} females. Table 1 shows that *Utx*^{KO} males were underrepresented in the progeny of this cross indicating that the loss of *Utx* is partially lethal for males. Significantly, no live *Utx*^{KO/KO} females were identified, indicating fully penetrant lethality.

To determine the time of lethality, embryos at different stages of gestation were isolated, characterized, and genotyped. Consistent with loss of embryos during gestation, we observed a high frequency of resorptions at embryonic day (E) 12.5 and E13.5 (Table 1). Importantly, only abnormal or partially resorbed *Utx*-null female embryos were detected at E11.5, and no live female

Author contributions: G.G.W. designed research; G.G.W. and S.M. performed research; R.A.Y. contributed new reagents/analytic tools; G.G.W., M.P.C., S.B., and A.W.C. analyzed data; and G.G.W. and R.J. wrote the paper.

The authors declare no conflict of interest.

Data deposition: The microarray and illumina sequencing data reported in this paper have been deposited in the Gene Expression Omnibus (GEO) database, www.ncbi.nlm.nih.gov/geo (accession no. GSE39222).

¹Present address: Hubrecht Institute for Developmental Biology and Stem Cell Research, Uppsalalaan 8, 3584CT, Utrecht, The Netherlands.

²To whom correspondence should be addressed. E-mail: jaenisch@wi.mit.edu.

This article contains supporting information online at www.pnas.org/lookup/suppl/doi:10.1073/pnas.1210787109/-DCSupplemental.

Table 1. UTX-deficiency leads to embryonic lethality for female embryos

Age	Males (% of males)			Females (% of females)			Reabsorbed (% of total)	Total
	<i>Utx^{Wt}</i>	<i>Utx^{KO}</i>	Subtotal	<i>Utx^{KO/Wt}</i>	<i>Utx^{KO/KO}</i>	Subtotal		
E8.5	3 (60)	2 (40)	5	4 (57)	3 (43)	7	0	12
E9.5	4 (50)	4 (50)	8	6 (50)	6 (50)	12	0	20
E10.5	11 (42)	15 (58)	26	10 (50)	10 (50)	20	0	46
E11.5	9 (53)	8 (47)	17	8 (75)	4 (25)	12	2 (6)	41
E12.5	4 (57)	3 (43)	7	6 (100)	0 (0)	6	8 (38)	21
E13.5	13 (65)	7 (35)	20	5 (100)	0 (0)	5	8 (24)	33
3 wk	79	15	94	61	0	61	N/A	155
Observed ratios	1	0.2		0.8	0			
Expected ratios	1	1		1	1			

This table provides a summary of observed progeny at different developmental time points obtained from matings between *Utx^{Fix}* males with a germ-line Cre deleter (*Ncre*) and *Utx^{KO/Wt}* females. Expected ratios and observed ratios are provided at the bottom with the latter calculated from the progeny genotyped at 3 wk of age. The timing of gestation was determined based on the morning of the appearance of a plug as being E0.5.

embryos were detected after E12.5 (Fig. 1A). This finding indicates that UTX deficiency in female, in contrast to male embryos leads to fully penetrant embryonic lethality. Upon closer examination of the abnormal E10.5 embryos we detected heart

malformations (although some of these embryos had heart muscle contractions) and neural tube closure defects. When embryos were isolated at E9.5, mutant female embryos displayed a delay in development as indicated by a reduced number of

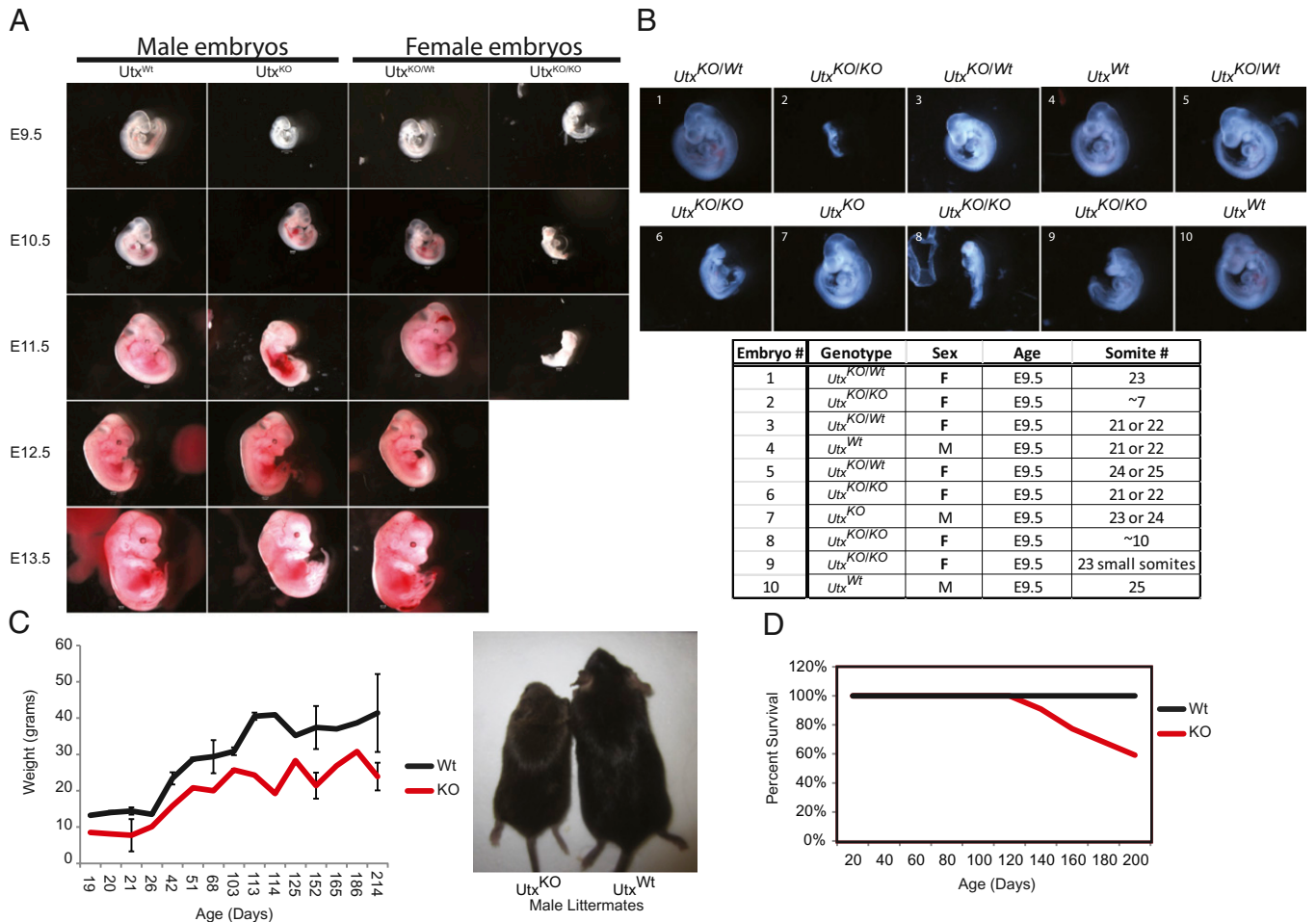


Fig. 1. UTX is required for development in a sex-specific manner. (A) *Utx* is required for development of female embryos. Representative embryos isolated at the respective time from a natural mating between a mutant male and heterozygote female (*Utx^{KO/Wt}*) are shown. All images are taken at the same magnification (8x) except for the E9.5 embryos, which were taken at a higher magnification (20x). **(B)** A representative litter from E9.5 that demonstrates the variability in phenotypes of *Utx*-null female embryos. **(C)** *Utx*-deficient males are smaller than wild-type males throughout their lifespan. Error bars represent the SD of the weights taken at that age. A representative image of a *Utx*-null male and wild-type littermate is shown. **(D)** *Utx*-deficient males die prematurely compared with wild-type littermates. The percent survival of wild-type ($n = 42$) and *Utx^{KO}* males ($n = 22$) followed for 200 d after birth.

somites and a failure to turn. Fig. 1*B* demonstrates the spectrum of defects in *Utx*-deficient sibling females obtained from a single litter. In contrast to *Utx* homozygous mutant female embryos, hemizygous mutant male embryos displayed a milder phenotype. At E9.5, *Utx*^{KO} males appeared relatively normal, but abnormalities were detected in some mutant embryos at E11.5. Importantly, however, normal appearing *Utx*^{KO} male embryos were observed at E13.5 and later stages of gestation, though at a lower than expected frequency, indicating some loss of mutant male embryos before E13.5. (Fig. 1*A* and Table 1). This result indicates that loss of both *Utx* copies in females results in a more severe phenotype than deletion of *Utx* in males.

Although at a significantly reduced frequency than expected, postnatal UTX-deficient males were viable (Table 1). These males were smaller than their littermates at birth and throughout adulthood (Fig. 1*C*), which could already be detected in utero (Fig. 1*A*). In addition, these animals had reduced survival compared with wild-type littermates (Fig. 1*D*). Although *Utx*^{KO} ES cells did not contribute to the germ line in chimeric animals, UTX-deficient males displayed normal spermatogenesis and were functionally fertile when mated with wild-type females or *Utx*^{KO/Wt} females (Fig. S2 and Table S1). Although it is possible that UTX plays a role in germ cell development as indicated by the *Utx*^{KO} ES-derived chimeras (none had germ-line transmission of the mutant allele), our data suggest that UTX is not required for male fertility. Together, it is clear that there exists a sex-specific requirement for UTX during development.

***Utx* Is Not Required for ES Cell Maintenance but Is Necessary for Proper Activation of Developmental Regulators.** To better understand the sex-specific loss of UTX mutant embryos, *Utx*^{KO} male, *Utx*^{KO/KO} female, and heterozygous *Utx*^{KO/Wt} female ES cells were isolated from the inner cell mass of explanted blastocysts. The three lines were derived from embryos of the same female, and the absence of UTX in the two mutant cell lines was confirmed by Western blot.

To determine whether UTX plays a role in maintaining the activity of key pluripotency genes, UTX-null male and female ES cells were grown under self-renewal conditions and stained for key pluripotency markers (Fig. S1*C*). The expression pattern of Oct3/4, Nanog, and SSEA-1 was unaffected by the loss of UTX. Similarly, we found that the deletion of UTX in ES cells did not affect the cell cycle and proliferation (Fig. S1*D*) of UTX-null ES cells. Thus, UTX does not play a role in ES cell self-renewal.

To investigate whether the loss of UTX has a critical role in differentiation, *Utx*^{KO} ES cells were tested in a teratoma formation assay. Two independent *Utx*^{KO} male ES cells (generated by in vitro targeting of existing V6.5 ES cells) and the two ES lines (*Utx*^{KO}, *Utx*^{KO/KO}) derived from explanted blastocysts were compared with *Utx*^{Flx}, *Utx*^{Wt}, and *Utx*^{KO/Wt} control ES cells for their ability to generate all three germ layers. For all of the in vitro assays performed, there was no observed difference in phenotype between *Utx*^{Flx} and *Utx*^{Wt} (V6.5) male ES cells. The teratomas derived from UTX-deficient ES cells displayed tissues from all three germ layers, consistent with UTX-null embryos surviving to midgestation (Fig. 2*A*). Of note, however, was the presence of a large number of giant trophoblast cells in the teratomas derived from the *Utx*^{KO/KO} female ES cells; these trophoblast cells were not present in the other teratomas analyzed.

We used the embryoid body assay to further investigate the differentiation capacity of UTX-deficient ES cells. *Utx*^{KO}, *Utx*^{KO/KO}, and *Utx*^{KO/Wt} ES cells were plated as hanging drops in media without LIF to form embryoid bodies, replated 2 d later on nonadherent plates and allowed to differentiate for 10 d. Interestingly, the in vivo sexual dimorphism appeared to be phenocopied: H&E sections revealed a diminished differentiation potential for *Utx*^{KO/KO} female ES cells compared with the male *Utx*^{KO} ES line. The heterozygous *Utx*^{KO/Wt} ES cells displayed typical differentiation potential based on the presence of complex structures in each of the EBs (Fig. 2*B*). Analysis of gene expression by quantitative PCR (qPCR) revealed

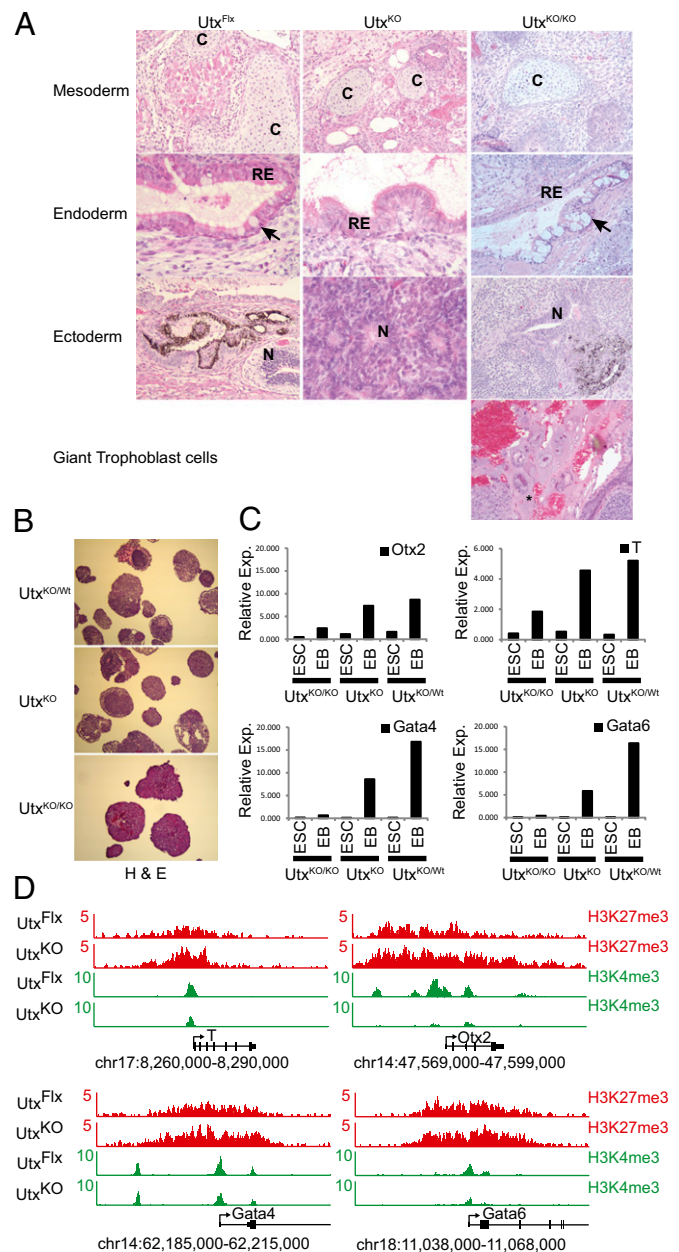


Fig. 2. *Utx* regulates the levels of H3K27me3 in ES cells and the timely activation of key developmental regulators during differentiation. (A) Representative pictures of the mesoderm, endoderm, and ectoderm structures observed in ES cell derived teratomas. *Utx*^{KO/KO} ES cell-derived teratomas contained a large number of giant trophoblast cells. Cartilage (C), Respiratory Epithelium (RE), neurons (N) and ciliated structure (Arrows) are indicated. (B) H&E staining of EBs harvested at day 10 postdifferentiation. Heterozygous female ES cells display structures indicative of differentiation in essentially all EBs in view. Female UTX-null ES cells do not. (C) Gene activation during embryoid body differentiation of male UTX-deficient (*Utx*^{KO}) male, UTX-deficient (*Utx*^{KO/KO}) female, and UTX-heterozygote (*Utx*^{KO/Wt}) female ES cells. qRT-PCR was performed on RNA harvested from ES cells and EBs collected at day 10. Fold activation over GAPDH is represented for four genes representing the three germ layers: mesoderm (*Gata4* and *Gata6*), endoderm (*T*), and ectoderm (*Otx2*). (D) H3K27me3 increases at developmental regulators in UTX-deficient ES cells. ChIP-seq density profiles for H3K27me3 and H3K4me3 in male *Utx*-null (*Utx*^{KO}) ES cells and male ES cells with restored UTX expression (*Utx*^{Flx}) are shown. The y axis floor is set at 0.5 reads per million. Gene models are shown below the density profiles.

that developmental regulators were not properly activated (Fig. 1B). Markers of all layers, endoderm (*Gata4* and *Gata6*), ectoderm (*Otx2*), and mesoderm (*T*) were analyzed and found to lack proper activation. In contrast, pluripotency genes such as *Nanog* and *Oct3/4* were appropriately silenced during differentiation. Although differences in gene expression were not observed for all developmental regulators tested, our data suggest that UTX is important for the correct and coordinated activation of several and that the loss of two copies of *Utx* in female ES cells has an increased affect over the loss of only one allele in male ES cells.

To exclude the possibility that UTX deficiency affects imprinting, the expression of all known imprinted genes was analyzed in UTX-null (*Utx^{KO/KO}*) and heterozygous (*Utx^{KO/Wt}*) female ES cells grown in self-renewal or differentiation conditions (+RA). No significant difference in the normalized expression was observed (Fig. S1E), indicating that abnormal imprinting is not a major cause for the difference in male and female mutant embryos. We also looked at whether the expression of UTY changes in the absence of UTX-deficient male embryos at E10.5. We performed quantitative PCR analysis on RNA harvested from the heads of wild-type and UTX-null male embryos and observed a slight decrease in UTY transcripts (Fig. S3A). Reduced embryo size or delayed development may explain the reduced level of UTY in the UTX-deficient male embryos.

Loss of UTX in Male ES Cells Results in a Genome-Wide Increase of H3K27me3. During ES cell differentiation, developmental regulators are activated, which coincides with the removal of H3K27me3 at their promoters. UTX is implicated in this process because it occupies the promoters of developmental genes during differentiation and the transient knockdown of UTX leads to an increase of H3K27me3 at these targets (6, 9). Consistent with this concept, UTX seems to be excluded from specific targets in ES cells under self-renewal conditions but is recruited to developmental regulators upon differentiation (8, 13). Interestingly, UTX can compete with PRC2 at the promoters of *Hox* genes in fibroblasts to regulate the steady state levels of H3K27me3 at these genes (9, 14). The possibility that UTX and PRC2 compete at promoters to regulate H3K27me3 levels in fibroblasts suggests that UTX may also function to modulate H3K27me3 at bivalent genes in ES cells.

To determine whether UTX has an unappreciated function in ES cells, we used chromatin immunoprecipitation followed by massively parallel DNA sequencing (ChIP-seq) and probed the deposition of H3K4me3 and H3K27me3 in male wild-type and male *Utx^{KO}* ES cells grown under self-renewal or differentiation conditions. Visual inspection of density profiles for H3K27me3 at representative genes revealed that H3K27me3 levels increased at transcription start sites (Fig. 2D). These genes also showed a slight decrease in H3K4me3. In contrast, the loss of UTX did not result in the presence of H3K27me3 at pluripotency genes, such as *Pou5f1*, indicating that the increase is specific to bivalent genes (Fig. S3A). Genome-wide, the average levels of H3K27me3 were significantly increased for all H3K27me3 target genes in the *Utx^{KO}* ES cells compared with *Utx^{Fix}* control cells, whereas the average levels of H3K27me3 at active genes were maintained (Fig. S3B). These data indicate that UTX regulates the levels of H3K27me3 in ES cells and this may affect their potential for differentiation.

UTX-Deficient ES Cells Are Responsive to Retinoic Acid (RA)-Induced Differentiation. To determine whether *Utx*-deficient ES cells are less responsive to differentiation as a result of the increased levels of H3K27me3 at developmental regulators, ChIP-seq analysis was performed on ES cells differentiated with RA. Previous reports have shown that UTX is required for gene activation following RA treatment by removing H3K27me3 (6, 9). *Utx^{KO}* and *Utx^{Fix}* ES cells were treated with RA for 48 h, crosslinked, and collected for ChIP-seq analysis. Consistent with previous reports showing that *Hox* genes are a UTX target during differentiation, the level of H3K27me3 in *Utx^{KO}* cells treated with RA was higher than that in wild-type controls (Fig. 3A). However, close inspection of the gene

tracks revealed that the levels of H3K27me3 in differentiated *Utx^{KO}* ES cells were lower than in undifferentiated *Utx^{KO}* ES cells, indicating active demethylation of H3K27me3 in the absence of UTX. Moreover, the levels of H3K4me3 increased at the promoters throughout the cluster, indicating that the genes were responsive to RA in the absence of UTX.

We performed a metagene analysis of the average levels of H3K27me3 of two different gene sets to investigate whether increased methylation was specific to the *Hoxb* cluster. The first group contained genes that maintained a bivalent state following RA treatment, and the second cluster comprised genes that resolved the bivalent domain by losing the H3K27me3 modification at their transcription start site. Consistent with our previous analyses, the average levels of H3K27me3 in *Utx^{KO}* ES cells grown under self-renewal conditions were higher for both gene sets (Fig. 3B). Additionally, the levels of H3K4me3 for both gene sets showed a slight but significant decrease in *Utx^{KO}* ES cells compared with *Utx^{Fix}* cells, which is in agreement with the chromatin state observed at individual gene tracks (Figs. 2D and 3A). The metagene analysis of “resolved” bivalent genes for *Utx^{KO}* ES cells treated with RA confirmed that *Utx*-deficient ES cells were responsive to RA as evidenced by both the reduction in the average H3K27me3 levels and increase in H3K4me3 levels for this group of genes (Fig. 3C). In contrast, the levels of H3K27me3 remained unchanged for genes that normally do not respond to RA in both the *Utx*-deficient and wild-type control cells.

To determine the effect of UTX deficiency on gene transcription, genome-wide analysis of gene expression was performed. RNA was isolated from *Utx^{KO}* and *Utx^{Fix}* ES cells grown in the presence or absence of RA and analyzed by microarrays. We focused analysis on the maintained and resolved categories of bivalent genes and found that the expression data were consistent with the ChIP-seq data. The bivalent genes that did not resolve the H3K27me3 mark showed no change in average normalized gene expression after RA exposure (Fig. 3D). In contrast, we observed an increase in the average normalized gene expression for the bivalent genes that had H3K27me3 removed in response to RA. The loss of UTX did not appear to affect transcriptional activation of resolved genes in response to RA (Fig. 3D). These data suggest that *Utx*-deficient ES cells are capable of responding to RA, indicating that compensatory mechanisms can replace the function of UTX under certain conditions.

Discussion

Since its discovery as an H3K27me3 demethylase, UTX has been hypothesized to play a critical role in resolving the poised state of developmental genes during differentiation (6, 8, 9). Our analysis of *Utx^{KO}* ES cells by ChIP-seq suggests the possibility that UTX acts to ensure optimal levels of H3K27me3 at bivalent genes, presumably by regulating the on/off rate of this modification. This model is in agreement with the suggestion that the steady state levels of H3K27me3 at transcription start sites is a result of a dynamic equilibrium between the opposing functions of UTX and PRC2 (14). Consistent with a role for UTX in counterbalancing PRC2 activity only at preexisting repressed regions, the deletion of *Utx* in ES cells did not result in increased levels of H3K27me3 at active genes such as the pluripotency genes, *Pou5f1* and *Nanog*. Furthermore, increased H3K27me3 at developmental regulators was associated with decreased H3K4me3 consistent with reinforced gene repression as a result of UTX deficiency.

While this work was being prepared for publication, Lee et al. (15) reported a requirement for UTX in cardiac development due to its ability to activate cardiac-specific genes in both a demethylase-dependent and -independent manner. Our analysis extends this conclusion and suggests that UTX has a more general role during development evidenced by observed neural tube closure defects and delayed turning of knockout embryos compared with wild-type embryos. It is unclear to what extent this phenotype is a consequence of UTX controlling the steady state levels of H3K27me3 as opposed to a function as an active demethylase involved in gene activation during cellular transitions. UTX can

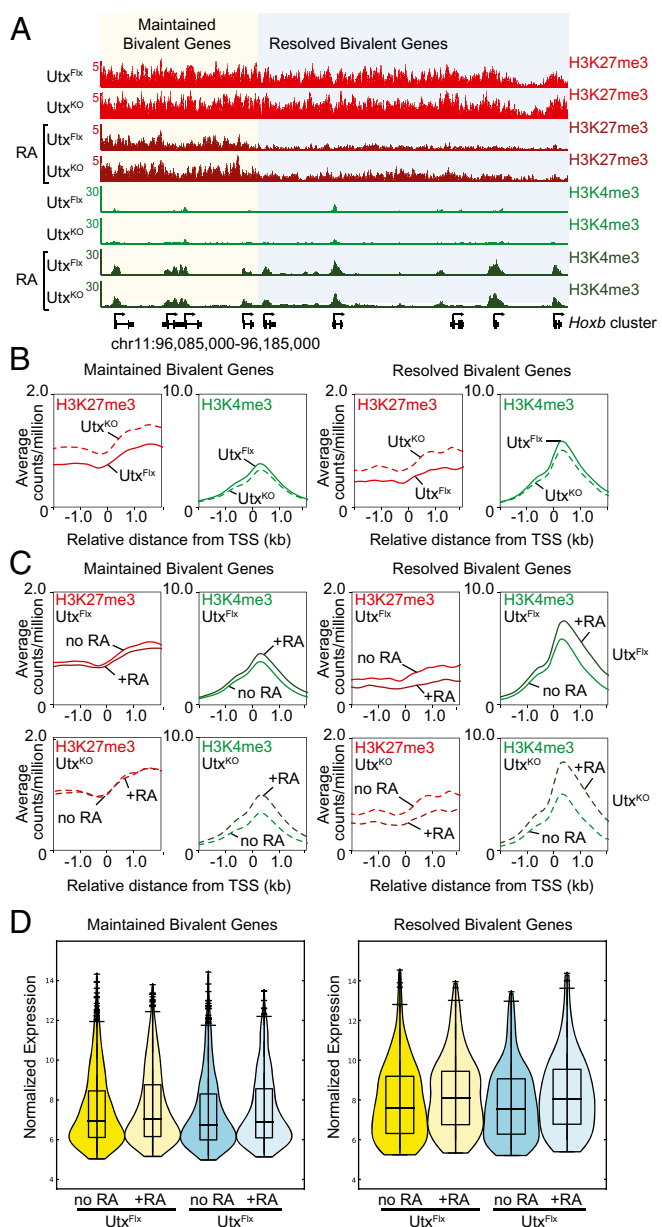


Fig. 3. UTX is not required for RA-induced differentiation. (A) Increased levels of H3K27me3 at the *Hoxb* cluster in the absence of UTX. H3K27me3 (red) and H3K4me3 (green) gene tracks for male ES cells with restored UTX expression (UTx^{Fix}) and *Utx*-null (UTx^{KO}) male ES cells that were untreated or treated with RA. During differentiation, bivalent genes can be maintained (yellow shading) or resolved (blue shading). Maintained bivalent genes are defined as those that maintain significant levels of H3K4me3 and H3K27me3 during RA-induced differentiation. Resolved bivalent genes are defined as genes that lost H3K27me3, but retained H3K4me3. The y axis floor is set at 0.5 reads per million. Gene models are shown below the density profiles. (B) Bivalent genes in UTX-deficient ES cells have increased levels of H3K27me3 and a reduction in H3K4me3. Metagene representations of the average H3K4me3 (green lines) and H3K27me3 (red lines) levels around transcription start sites (± 2 kb) for wild-type (solid lines) and *Utx*-deficient (dashed lines) ES cells. (C) Demethylation of H3K27me3 in UTX-deficient ES cells in response to RA. Metagene representations of the average H3K4me3 (green lines) and H3K27me3 (red lines) levels around transcription start sites (± 2 kb) for wild-type (solid lines) and *Utx*-deficient (dashed lines) ES cells. H3K27me3 levels are reduced at resolved genes for both wild-type and UTX-deficient ES cells. (D) UTX-deficient male ES cells are transcriptionally responsive to RA. Violin plots summarizing the gene expression of wild-type (UTx^{Fix}) and UTX-deficient (UTx^{KO}) ES cells grown in self-renewal conditions (no RA) or under differentiation conditions (+RA). Maintained and resolved bivalent genes were analyzed.

associate with the H3K4 methyltransferase complex containing the core subunits MLL3 or MLL4, ASH2L, WDR5, and RBBP5, and it is believed that this allows for the coordinated methylation of H3K4me3 and H3K27me3 demethylation from the TSS of target genes (16). Evidence points to a critical role for this complex in gene activation downstream of nuclear receptors such as the Farnesoid X or RA receptor (16–24). UTX can also interact with Brg1 and T box transcription factors to modulate gene activity in a demethylase-independent manner (15, 25). The exact nature of UTX involvement and its requirement for gene activation during differentiation is still unclear because most biochemical analysis has been performed in fibroblast cell lines. Here, we demonstrate that UTX is not required for H3K27me3 demethylation during ES cell differentiation by RA, suggesting that compensatory mechanisms can replace UTX function under certain conditions. Consistent with this notion, JMJD3 has been shown to respond downstream of RA in developing neurons, indicating that it may also play a compensatory role in response to RA-induced differentiation of *Utx*-null ES cells (26, 27). To tease out the precise role of UTX during development, it will be important to generate tissue-specific knockout animals.

Whereas UTX-deficient females died before E12.5, ~20% of hemizygous male mutant embryos survived to adulthood, suggesting that UTY can compensate for the loss of UTX. UTY has no known enzymatic activity, indicating that its main function might be to recruit, in a similar fashion as UTX, Brg1-containing Swi/Snf complexes and T box transcription factors to specific genes during differentiation. Whether the partial rescue can be explained solely by a demethylase-independent function remains to be determined. It is feasible that UTY might have enzymatic activity *in vivo* under specific conditions. Recently, the crystal structure of the enzymatic domain of UTX was solved and revealed important information regarding the amino acid requirements for its specific activity (12). The most critical residues for H3K27me3 demethylation are present in the catalytic domain of UTY, suggesting that indeed UTY may be an active demethylase. To determine with certainty the nature of UTY biology *in vivo*, a *Uty* knockout model would be valuable. However, conventional methods for gene targeting have been unsuccessful for genes on the Y chromosome making *in vivo* loss of function studies difficult to perform. It remains to be seen whether advances in gene targeting can overcome some of these challenges (28, 29). Nevertheless, our data indicate an important role for UTY during development.

In conclusion, our data suggest that UTX may counterbalance polycomb activity by regulating H3K27me3 at developmental regulators in ES cells. Because UTX is ubiquitously expressed, it is possible that the enzyme has a similar function in adult stem cells to ensure tissue homeostasis. *Utx* mutations have been identified in several cancers, suggesting a role as a tumor suppressor (30–36). The aberrant regulation of H3K27me3 seems to be an important step in cancer development because *Ezh2*, the enzyme that deposits H3K27me3, is an established oncogene (37). It is conceivable, therefore, that somatic cells that acquire inactivating *Utx* mutations lose, similar to *Utx*-null ES cells, the ability to regulate H3K27me3 across the genome, which may predispose cells to tumorigenesis.

Experimental Procedures

Generation of *Utx*-Targeted ES Cells. A “knockout-first” targeting vector for the *Utx* allele was obtained from the European knockout consortium (EUCOMM) to generate *Utx*-deficient and conditional ES cells. The targeting construct, shown in Fig. S1A, contains a splice acceptor β -geo cassette flanked by two Flp sites preceding the third exon of the *Utx* allele. In addition, the targeting construct introduces two loxP sites on either side of exon 3, allowing for conditional ablation of the exon upon the addition of cre recombinase. The Flp sites flanking the splice acceptor β -geo cassette allow for its removal after the addition of the flipase enzyme resulting in the generation of a conditional allele. V6.5 ES cells (38) were electroporated, Neo^R colonies were screened by PCR, and several independently targeted lines were obtained. To generate UTx^{Fix} and UTx^{KO} ES cell lines, multiple independently targeted clones were electroporated with puro^R expression vectors that express either Flpase (UTx^{Fix}) or Cre (UTx^{KO}). To confirm that

targeting of the *Utx* allele resulted in the elimination of *Utx* transcript and protein, quantitative RT-PCR and Western blot analysis was performed. ES cell lines that were targeted with the full targeting construct displayed hypomorphic expression of *Utx* with ~50% of mRNA transcripts than the parental v6.5 ES cells (Fig. S1B). As expected, when these hypomorphic lines were exposed to Cre, the remaining transcripts were eliminated, resulting in the ablation of protein. When the hypomorphic lines were treated with Flpase, the normal levels of *Utx* mRNA were restored.

Derivation of ES Cells. Following protocols described in ref. 39, ES cells were isolated from blastocyst embryos using ESC derivation media: KOSR (knock-out serum replacement, Gibco, catalog no. 1028-028), LIF ESGRO (1× 107 units of ESGRO per mL; Chemicon, catalog no. ESG1106), Mek1 inhibitor (PD98059; Cell Signaling Technology, catalog no. 9900), nonessential amino acids, glutamine solution, and pen/strep solution. Blastocysts were obtained from a *Utx*^{KO/wt} female crossed with a NestinCre⁺/*Utx*^{Flx} male. This first step of trypsinization was considered passage 1.

Mouse Blastocyst Injections and Teratoma Formation. All animal procedures were performed according to National Institutes of Health guidelines and were approved by the Committee on Animal Care at the Massachusetts Institute of Technology. B6D2F2 blastocysts were injected with *Utx*^{Flx}, *Utx*^{Hyp}, or *Utx*^{KO} ES cells (V6.5 is parental line) and transferred to Swiss pseudo-pregnant females. Resulting chimeras were identified by agouti coat color, and germ-line transmission was verified by breeding of the chimera(s) to C57BL/6 females. Teratoma formation was performed by depositing 1 × 10⁶ cells under the flanks of recipient SCID or *Rag2*^{-/-} mice. Tumors were isolated 3–6 wk later for histological analysis.

Differentiation of ES Cells. Embryoid body. ES cells were trypsinized, preplated, and resuspended in ES medium minus LIF at 10⁴ cells per mL. Twenty-microliter drops were placed onto the lid of a bacterial plate, inverted, and

incubated for 2 d at 37 °C. The hanging drops were put into suspension culture in a bacterial plate and incubated for an additional 8 d.

RA differentiation. ES cells were trypsinized and plated on gelatin in ES media (+LIF). The next day, the media was replaced with ES media minus LIF plus 1 × 10⁻⁷ M RA. Cells were cultured for an additional 48 h with one media exchange.

Generation of Hemizygous Mutant Males. To generate *Utx*^{KO} animals, a well characterized NestinCre transgenic strain was used to generate 1lox alleles in the germ line (40, 41). *Utx*^{Hyp} or *Utx*^{Flx} animals were crossed with the NestinCre strain to generate conditional *Utx*^{KO} male animals. The males were fertile, transmitted an *Utx*^{KO} allele to their progeny, and gave rise to *Utx*^{KO}/*Utx*^{wt} females when crossed with wild-type females.

ChIP-Seq Experiments. *Utx*^{KO} ES cells and *Utx*^{Flx} ES cells were grown in 15-cm plates on gelatin in either ES cell media + LIF or ES cell media without LIF but with 1 μM of RA. After treatment with RA for 48 h, a fraction of cells that were not crosslinked was harvested for RNA isolation and gene expression analysis; the remaining cells were chemically crosslinked. Chromatin immunoprecipitation was performed using antibodies versus H3K27me3 (Abcam) and H3K4me3 (Millipore). Detailed procedures can be found in *SI Experimental Procedures*. Illumina/Solexa sequence preparation, sequencing, and quality control were provided by Illumina. A brief summary of the technique and minor protocol modifications as well as data analysis are described in *SI Experimental Procedures*. Data sets have been deposited in the Gene Expression Omnibus (<http://www.ncbi.nlm.nih.gov/geo/>).

ACKNOWLEDGMENTS. We thank Ruth Flannery, Jessica Dausman, Kibibi Ganz, and Peter Ros for support with animal care and experiments. We thank Dong Dong Fu and Qing Gao for their assistance with pathology, Jeong-Ah Kwon for help with microarray, and Kevin Thai for help with sequencing experiments. This work was supported by National Institutes of Health Grants 5-F32-F32HD055038 and R37-HD045022.

- Guenther MG, Levine SS, Boyer LA, Jaenisch R, Young RA (2007) A chromatin landmark and transcription initiation at most promoters in human cells. *Cell* 130:77–88.
- Cao R, et al. (2002) Role of histone H3 lysine 27 methylation in Polycomb-group silencing. *Science* 298:1039–1043.
- Czermin B, et al. (2002) Drosophila enhancer of Zeste/ES complexes have a histone H3 methyltransferase activity that marks chromosomal Polycomb sites. *Cell* 111:185–196.
- Bernstein BE, et al. (2006) A bivalent chromatin structure marks key developmental genes in embryonic stem cells. *Cell* 125:315–326.
- Jaenisch R, Young R (2008) Stem cells, the molecular circuitry of pluripotency and nuclear reprogramming. *Cell* 132:567–582.
- Agger K, et al. (2007) UTX and JMJD3 are histone H3K27 demethylases involved in HOX gene regulation and development. *Nature* 449:731–734.
- Hong S, et al. (2007) Identification of JmjC domain-containing UTX and JMJD3 as histone H3 lysine 27 demethylases. *Proc Natl Acad Sci USA* 104:18439–18444.
- Lan F, et al. (2007) A histone H3 lysine 27 demethylase regulates animal posterior development. *Nature* 449:689–694.
- Lee MG, et al. (2007) Demethylation of H3K27 regulates polycomb recruitment and H2A ubiquitination. *Science* 318:447–450.
- Greenfield A, et al. (1998) The UTX gene escapes X inactivation in mice and humans. *Hum Mol Genet* 7:737–742.
- Xu J, Deng X, Watkins R, Distche CM (2008) Sex-specific differences in expression of histone demethylases Utx and Uty in mouse brain and neurons. *J Neurosci* 28:4521–4527.
- Sengoku T, Yokoyama S (2011) Structural basis for histone H3 Lys 27 demethylation by UTX/KDM6A. *Genes Dev* 25:2266–2277.
- Wang JK, et al. (2010) The histone demethylase UTX enables RB-dependent cell fate control. *Genes Dev* 24:327–332.
- Swigut T, Wysocka J (2007) H3K27 demethylases, at long last. *Cell* 131:29–32.
- Lee S, Lee JW, Lee SK (2011) UTX, a histone H3-lysine 27 demethylase, acts as a critical switch to activate the cardiac developmental program. *Dev Cell* 22:25–37.
- Issaeva I, et al. (2007) Knockdown of ALR (MLL2) reveals ALR target genes and leads to alterations in cell adhesion and growth. *Mol Cell Biol* 27:1889–1903.
- Cho YW, et al. (2007) PTIP associates with MLL3- and MLL4-containing histone H3 lysine 4 methyltransferase complex. *J Biol Chem* 282:20395–20406.
- Ananthanarayanan M, et al. (2011) Histone H3K4 trimethylation by MLL3 as part of ASCOM complex is critical for NR activation of bile acid transporter genes and is downregulated in cholestasis. *Am J Physiol Gastrointest Liver Physiol* 300:G771–G781.
- Kim DH, Lee J, Lee B, Lee JW (2009) ASCOM controls farnesoid X receptor transactivation through its associated histone H3 lysine 4 methyltransferase activity. *Mol Endocrinol* 23:1556–1562.
- Lee J, et al. (2009) A tumor suppressive coactivator complex of p53 containing ASC-2 and histone H3-lysine-4 methyltransferase MLL3 or its paralogue MLL4. *Proc Natl Acad Sci USA* 106:8513–8518.
- Lee J, et al. (2008) Targeted inactivation of MLL3 histone H3-Lys-4 methyltransferase activity in the mouse reveals vital roles for MLL3 in adipogenesis. *Proc Natl Acad Sci USA* 105:19229–19234.
- Lee S, et al. (2009) Crucial roles for interactions between MLL3/4 and INI1 in nuclear receptor transactivation. *Mol Endocrinol* 23:610–619.
- Lee S, Lee J, Lee SK, Lee JW (2008) Activating signal cointegrator-2 is an essential adaptor to recruit histone H3 lysine 4 methyltransferases MLL3 and MLL4 to the liver X receptors. *Mol Endocrinol* 22:1312–1319.
- Lee S, Roeder RG, Lee JW (2009) Roles of histone H3-lysine 4 methyltransferase complexes in NR-mediated gene transcription. *Prog Mol Biol Transl Sci* 87:343–382.
- Miller SA, Mohn SE, Weinmann AS (2010) Jmjd3 and UTX play a demethylase-independent role in chromatin remodeling to regulate T-box family member-dependent gene expression. *Mol Cell* 40:594–605.
- Dai JP, Lu JY, Zhang Y, Shen YF (2010) Jmjd3 activates Mash1 gene in RA-induced neuronal differentiation of P19 cells. *J Cell Biochem* 110:1457–1463.
- Jepsen K, et al. (2007) SMRT-mediated repression of an H3K27 demethylase in progression from neural stem cell to neuron. *Nature* 450:415–419.
- Hockemeyer D, et al. (2009) Efficient targeting of expressed and silent genes in human ESCs and iPSCs using zinc-finger nucleases. *Nat Biotechnol* 27:851–857.
- Hockemeyer D, et al. (2011) Genetic engineering of human pluripotent cells using TALE nucleases. *Nat Biotechnol* 29:731–734.
- Dalglish GL, et al. (2010) Systematic sequencing of renal carcinoma reveals inactivation of histone modifying genes. *Nature* 463:360–363.
- Gui Y, et al. (2011) Frequent mutations of chromatin remodeling genes in transitional cell carcinoma of the bladder. *Nat Genet* 43:875–878.
- Jankowska AM, et al. (2011) Mutational spectrum analysis of chronic myelomonocytic leukemia includes genes associated with epigenetic regulation: UTX, EZH2, and DNMT3A. *Blood* 118:3932–3941.
- Morin RD, et al. (2010) Somatic mutations altering EZH2 (Tyr641) in follicular and diffuse large B-cell lymphomas of germinal-center origin. *Nat Genet* 42:181–185.
- Staller P (2010) Genetic heterogeneity and chromatin modifiers in renal clear cell carcinoma. *Future Oncol* 6:897–900.
- van Haaften G, et al. (2009) Somatic mutations of the histone H3K27 demethylase gene UTX in human cancer. *Nat Genet* 41:521–523.
- Wartman LD, et al. (2011) Sequencing a mouse acute promyelocytic leukemia genome reveals genetic events relevant for disease progression. *J Clin Invest* 121:1445–1455.
- Margueron R, Reinberg D (2011) The Polycomb complex PRC2 and its mark in life. *Nature* 469:343–349.
- Eggan K, et al. (2001) Hybrid vigor, fetal overgrowth, and viability of mice derived by nuclear cloning and tetraploid embryo complementation. *Proc Natl Acad Sci USA* 98:6209–6214.
- Markoulaki S, Meissner A, Jaenisch R (2008) Somatic cell nuclear transfer and derivation of embryonic stem cells in the mouse. *Methods* 45:101–114.
- Bates B, et al. (1999) Neurotrophin-3 is required for proper cerebellar development. *Nat Neurosci* 2:115–117.
- Dubois NC, Hofmann D, Kaloulis K, Bishop JM, Trumpp A (2006) Nestin-Cre transgenic mouse line Nes-Cre1 mediates highly efficient Cre/loxP mediated recombination in the nervous system, kidney, and somite-derived tissues. *Genesis* 44:355–360.